land

MDPI

Article

The Loss and Recovery Potential of Net Ecosystem Productivity in Mining Areas: A Global Assessment Based on Data for 2000–2020

Yongjun Yang [1], Renjie Gong [1], Shuaihui Liu [1], Qinyu Wu [2,*] and Fu Chen [3]

[1] School of Environment and Spatial Informatics, China University of Mining and Technology, Xuzhou 221116, China; y.yang@cumt.edu.cn (Y.Y.); rj.gong@cumt.edu.cn (R.G.); liushuaihui@cumt.edu.cn (S.L.)
[2] School of Social & Environmental Sustainability, University of Glasgow, Dumfries DG1 4ZL, UK
[3] School of Public Administration, Hohai University, Nanjing 211100, China; chenfu@hhu.edu.cn
* Correspondence: qinyu.wu@glasgow.ac.uk

Abstract: Climate change control requires more land to increase ecosystem carbon sequestration. With the high-intensity development of mineral resources in past decades, massive mining areas have been generated worldwide. However, few studies have evaluated the carbon sequestration of these mining areas. In this study, we analyzed the net ecosystem productivity (NEP) changes and calculated the NEP losses in global terrestrial mining areas. We adopted the random forest model to evaluate the NEP recovery potential and its driving factors. The key findings are that (1) the NEP of global mining areas exhibited a relatively obvious decreasing trend from 2000 to 2020, with an overall reduction of 29.1% and a maximum decline of 35.7%. By 2020, the NEP loss in mining areas was 11.9 g C m^{-2} $year^{-1}$, and the total loss reached 576.9 Gg C $year^{-1}$. (2) Global mining areas demonstrate significant NEP recovery potential, with an average of 12.0 g C m^{-2} $year^{-1}$. Notably, Oceania and South America have significantly higher recovery potentials, with average mine site NEP recovery potentials of 15.9 g C m^{-2} $year^{-1}$ and 16.1 g C m^{-2} $year^{-1}$. In contrast, European mines have considerably lower recovery potentials of less than 10 g C m^{-2} $year^{-1}$. In Asia, North America and Africa, the NEP recovery potential varies widely from mine to mine, but generally meets the global average. (3) The annual precipitation, population density, organic soil carbon, and average slope are important drivers of NEP recovery in mining areas and exhibit positive correlations with the NEP recovery potential. In contrast, mine area and minimum temperature exhibit a negative correlation. The dependency curves of the three drivers, standardized precipitation evapotranspiration index, average elevation, and annual maximum temperature, are U-shaped, indicating that the recovery potential was poorer in the tropical and frigid zones with less precipitation. The results of this study provide a scientific basis for ecological restoration and sustainable development of mining areas worldwide.

Keywords: ecological restoration; remote sensing; mining; net ecosystem productivity; random forest model

check for updates

Citation: Yang, Y.; Gong, R.; Liu, S.; Wu, Q.; Chen, F. The Loss and Recovery Potential of Net Ecosystem Productivity in Mining Areas: A Global Assessment Based on Data for 2000–2020. *Land* **2024**, *13*, 1913. https://doi.org/10.3390/land13111913

Academic Editor: Guillermo J. Martinez-Pastur

Received: 11 October 2024
Revised: 9 November 2024
Accepted: 13 November 2024
Published: 14 November 2024

Copyright: © 2024 by the authors. Licensee MDPI, Basel, Switzerland. This article is an open access article distributed under the terms and conditions of the Creative Commons Attribution (CC BY) license (https://creativecommons.org/licenses/by/4.0/).

1. Introduction

Since the industrial revolution, the influence of human society on Earth's ecosystems has intensified and become more profound, resulting in a continuous increase in global CO_2 concentrations, gradual global warming, and significant disruption of the carbon cycle and biodiversity within ecosystems. These alterations pose substantial threats to human health and socio-economic stability [1,2]. The Kyoto Protocol established during the United Nations Framework Convention on Climate Change [3] acknowledges the critical role of terrestrial ecosystems in the global carbon cycle, and it advocates for the protection, enhancement, and quantification of the terrestrial biosphere's capacity to sequester anthropogenic CO_2 emissions. Vegetation, as an integral component of terrestrial ecosystems, plays a crucial role by absorbing CO_2 through photosynthesis. This process

enhances the carbon sequestration capacity, reduces atmospheric CO_2 concentrations, and mitigates global warming. Thus, it is essential for achieving ecological sustainability and carbon balance [4,5]. The net ecosystem productivity (NEP) quantifies the net carbon flux within an ecosystem and is defined as the difference between the carbon assimilated through photosynthesis (CO_2 uptake) and the carbon lost via plant and soil respiration. Assessing the NEP is crucial for determining whether an ecosystem functions as a carbon source or a carbon sink. A negative NEP value signifies a carbon source, while a positive value denotes a carbon sink [6,7]. Consequently, the NEP is of paramount importance for quantifying ecosystem carbon sequestration and elucidating carbon cycle mechanisms, thereby facilitating more effective monitoring and regulation of CO_2 absorption, storage, and release processes.

In recent years, with the increasing frequency and intensity of human activities, the exploitation of mineral resources has significantly accelerated, becoming a major cause of land degradation. The extraction, transportation, processing, and utilization of mineral resources not only lead to surface deformation and the creation of land damage but also alter the original vegetation types of the region [8,9]. This can disrupt the local ecological balance and result in environmental degradation. Currently, numerous studies have emphasized the environmental and social impacts of mining, which are often attributed to land degradation [10,11], loss of biodiversity [12,13], and livelihood displacement [14]. Given the ecological and environmental issues arising from mining activities, restoring degraded ecosystems in mining areas is crucial for achieving sustainable development. To achieve this goal, it is imperative to enhance the monitoring and management of mining ecological environments [15]. Particularly in the context of climate change, it is essential to conduct in-depth research on the carbon exchange capacity between the atmosphere and terrestrial ecosystems in mining areas. This will help address the challenges posed by the uncertainties in ecosystem carbon sequestration and promote ecosystem restoration and sustainable environmental development.

The research on global NEP in mining areas is still in its early stages. Although existing studies have assessed vegetation loss in mines and developed monitoring methods such as remote sensing and ground surveys, the long-term impacts of mining activities on the environment, vegetation cover, and ecosystem health require further exploration. Mining activities typically occur over large areas and have long-lasting negative environmental impacts. For example, Latifovic et al. [16] used Landsat and Advanced Very High-Resolution Radiometer data to study land cover changes in the Athabasca oil sands region of Canada and found that over 700 hectares of vegetation had degraded from 1992 to 2001, with a slight decline in vegetation greenness and increased temperatures from 1990 to 2002. Waring et al. [17] utilized the MODIS Global Disturbance Index to detect disturbances in woody ecosystems, demonstrating its effectiveness in monitoring large-scale ecosystem disturbances. Ma et al. [18] combined precipitation data and the MODIS Enhanced Vegetation Index to develop a Vegetation Disturbance Index to distinguish disturbances, applying the Vegetation Disturbance Index to the Mongolian Plateau from 2000 to 2015.

Despite several studies on the impact of mining-induced disturbances on vegetation, research focusing on changes in carbon sink capacity due to vegetation destruction is still scarce [19]. Coal mining can directly and indirectly affect the carbon sequestration effect of vegetation, complicating the calculation of biomass and carbon loss caused by mining, as well as quantifying changes in vegetation carbon sequestration in mining areas. Existing studies have estimated changes of net primary productivity in mining areas, using models like the Carnegie–Ames–Stanford Approach and ecological parameters to analyze the variations of net primary productivity. For instance, Xu et al. [20]. and Hou et al. [21]. conducted relevant studies on different mining areas [22]. However, these analyses often focus on individual mining areas, yielding insights limited to small-scale regions. Several studies have sought to quantify the recovery potential of mining in a range of ecosystems. For example, research in reclaimed mine areas, such as forests and grasslands, has shown that effective soil and vegetation management can restore carbon levels close to those of

undisturbed ecosystems. In Ohio, reclaimed pasture soils achieved SOC levels comparable to forest soils after 25 years, indicating that long-term, systematic management can enhance carbon sequestration [23]. Similarly, research in tropical mining areas has shown increased soil CO_2 fluxes in reclaimed lands, which implies higher carbon exchange and activity following successful reclamation. These findings emphasize the potential for NEP recovery in degraded mining areas through targeted ecological restoration practices [24].

Globally, more research has been attempting to map the geographical distribution of mining areas. Sonter et al. [22] used a database of mining and deposit locations and applied buffers around these points to estimate areas potentially affected by mining. They found that 62,381 mining and deposit locations globally may impact 50 million square kilometers of the Earth's surface, with 8% overlapping with protected areas, 7% overlapping with key biodiversity areas, and 16% overlapping with the remaining wilderness. Werner et al. [25] directly studied mining areas using satellite data and finely delineated the boundaries of 295 major mining areas, covering a total area of approximately 3633 km^2. Maus et al. [26] employed a similar visual interpretation method and applied a roughly 10 km buffer to delineate over 6000 mining areas, generating 21,060 polygons that cover about 57,277 km^2. These studies highlight the global threats that mining poses to ecosystems. Nonetheless, existing research lacks a comprehensive assessment of the loss of NEP and the potential for recovery in global mining areas. Future studies should further quantify carbon loss in mining areas and explore effective restoration measures to mitigate the impacts of mining on global ecosystems.

Therefore, in this study we assessed the NEP loss and recovery potential in global mining areas. The primary research objectives were (1) to analyze the changes in NEP across global mining areas, (2) to evaluate the NEP loss in these areas, (3) to assess the recovery potential and discuss the factors influencing this potential, and (4) to provide insights for the management of mining ecosystems. The results of this study provide a scientific basis for the ecological restoration and sustainable development of mining areas worldwide.

2. Materials and Methods

2.1. Data Sources

2.1.1. Global Mining Areas

The mining area dataset at the global scale used was obtained from the website of the Environmental Science Data Release (http://pangaea.de) (Accessed on 10 September 2024). This dataset provides spatially explicit estimates of the areas directly used for mining on a global scale and does not cover all existing mining areas globally, but it includes most mining areas, mainly for coal and metal ores. This dataset identifies the vector boundaries of the mining areas through a combination of high-resolution satellite imagery provided by Sentinel-2 (de-clouded), Bing Imagery, and Google Satellite, including areas such as mining pits, tailings dams, waste rock dumps, ponds, and mine processing infrastructure. The overall accuracy of the mining area extraction is 88.4% [27]. The dataset has some limitations, such as potential omissions of smaller or less detectable sites, which could slightly underrepresent mining areas, particularly in regions with complex land uses. Additionally, minor boundary inaccuracies may exist due to the resolution limits of satellite data. Despite these limitations, it provides the most comprehensive information on global mining land use [27]. We screened out the mine sites with areas greater than or equal to 1 km^2. Therefore, 14,546 mining areas with valid data were retained in this study (Figure 1).

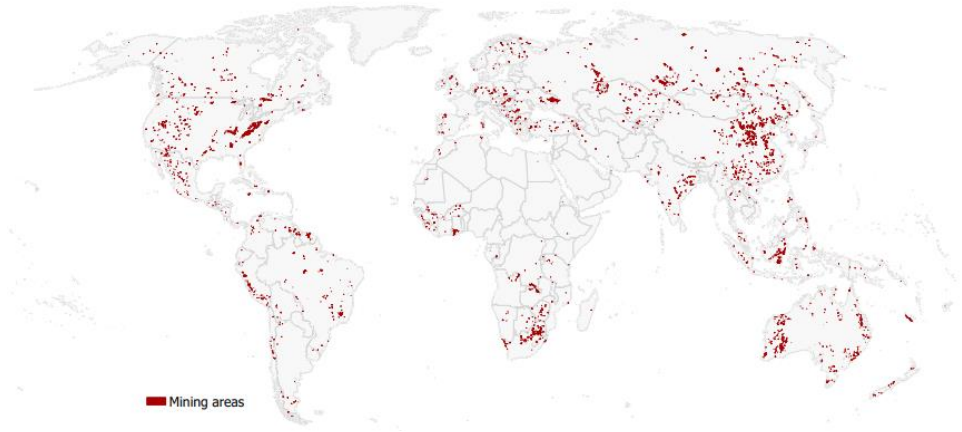


Figure 1. Global mining areas.

2.1.2. Net Ecosystem Productivity

The NEP is the gross primary productivity (the amount of organic carbon fixed by organisms through photosynthesis per unit of time) after deducting the portion consumed via respiration of autotrophic organisms and the photosynthetic products consumed via respiration of heterotrophic organisms (soil respiration). The global NEP dataset we used was obtained from the National Earth System Science Data Center (http://www.geodata.cn) (Accessed on 10 September 2024). This dataset provides global net ecosystem productivity data for terrestrial ecosystems for 2000–2020 and contains latitude and longitude information for the data, with a spatial resolution of 500 m, a temporal resolution of 1 year, and units of g C m^{-2} $year^{-1}$ [28]. This dataset was combined with net ecosystem carbon exchange data from the global flux network and data for environmental factors affecting the spatial and temporal variations in the net ecosystem carbon exchange to estimate the monthly net ecosystem carbon exchange at the global flux site scale using a data-driven machine-learning model. Then, the data-driven model constructed at the site scale was used to obtain the global-scale monthly net ecosystem carbon exchange by combining the data for the predictor variables of the spatial grids and taking the negative of it to obtain the monthly NEP. Finally, the monthly NEP was accumulated to the year to obtain the annual NEP. The final data accuracy of the 500 m monthly net ecosystem carbon exchange estimation has an R^2 value of 0.72 for five-fold independent cross-validation and a root mean square error of 0.96 g C m^{-2} day^{-1}. Additionally, spatial and temporal resolution constraints can introduce minor uncertainties, especially in smaller or heterogeneous land use areas. Despite these limitations, the dataset remains robust and is a unique choice for evaluating large-scale NEP trends and recovery potential across global mining areas.

2.1.3. Influencing Factors

To assess the factors influencing the NEP in mining areas, 11 relevant indicators from the climatic, ecological, and economic aspects were selected (Table 1). These indicators were carefully chosen to capture the multifaceted drivers of NEP and to provide a comprehensive basis for evaluating the NEP recovery potential of the mining areas.

For climatic factors, we used the standardized precipitation evapotranspiration index, annual rainfall, and the maximum and minimum temperatures in the mining area. The standardized precipitation evapotranspiration index represents the deviation of the current climate equilibrium (precipitation minus evapotranspiration potential) from the long-term equilibrium in the form of a standardized variable (mean zero, unit variance), and the larger the value of the standardized precipitation evapotranspiration index, the wetter it is. The standardized precipitation evapotranspiration index data we have selected come from the SPEIbase dataset [29], which provides standardized precipitation evapotranspiration index data on 1–48 month time scales from 1901–2021. In this dataset, the reference period calculated corresponds to the entire study period. The global precipitation and maximum

and minimum temperature data are obtained from the National Earth System Science Data Center (http://www.geodata.cn) (Accessed on 10 September 2024), where the rainfall dataset provides annual cumulative precipitation raster data on a global scale, which is generated by computational simulation of the worldclim rainfall data. The global maximum and minimum temperature datasets are derived from the worldclim monthly maximum and monthly minimum temperature data, which are computed in the R language, and the accuracy is maintained after processing.

For ecological factors, we have employed the average gross primary production within the 2 km buffer zone of the mine, the soil organic carbon content, average elevation and average slope of the mining area for measurement. Gross primary production is the amount of organic carbon fixed by organisms (mainly green plants) through photosynthesis per unit time, which describes the amount of carbohydrates produced by plants synthesizing CO_2. Gross primary production data come from the dataset VODCA2GPP [30], which is based on the novel sink-driven gross primary production estimation methodology proposed by Teubner et al. [31,32]. It utilizes a new merged-frequency vegetation optical-depth climate archive in conjunction with the ERA5-Land Temperature data to generate a coherent long-term global gross primary production data record. Global soil organic carbon data were obtained from the GloSIS platform (Global Soil Information System of the FAO Global Soil Partnership, https://data.apps.fao.org/glosis) (Accessed on 10 September 2024). The GSOCmap provided by this platform is the first ever global soil organic carbon map produced through a consultative and participatory process among member countries. The digital elevation model data were obtained from the Global Ocean and Land Terrain Models (GOTM) provided by GEBCO (https://www.gebco.net) (Accessed on 10 September 2024), a dataset that provides a global terrain model for the oceans and land. And the slope data we used were also calculated from this digital elevation model data.

In terms of economic factors, we have employed the mine area, population density, and the gross domestic product of the mining area, where the mine area is calculated from the mine vector boundaries. Population density data were obtained from the GHSL-Global Human Settlement Layer (http://ghsl.jrc.ec.europa.eu/index.php) (Accessed on 10 September 2024), which provides population datasets with global 100 m resolution from 2000–2020. Gross domestic product data were obtained from the Chen and Gao [33] published dataset, which provides gridded revised real gross domestic product data for the years 1992–2019 globally.

Table 1. Indicators used in NEP recovery potential assessment.

Type of Indicator	Indicator	Units	Data Sources
Climate indicators	Standardized precipitation evapotranspiration index	Standard deviation	SPEIbase dataset
	Annual precipitation	Mm	http://www.geodata.cn (Accessed on 10 September 2024)
	Maximum temperature	°C	http://www.geodata.cn (Accessed on 10 September 2024)
	Minimum temperature	°C	http://www.geodata.cn (Accessed on 10 September 2024)
Ecological indicators	Average gross primary productivity within the 2 km buffer zone of mining area	kg C m^{-2} $year^{-1}$	VODCA2GPP dataset
	Soil organic carbon	kg m^{-3}	https://data.apps.fao.org/glosis (Accessed on 10 September 2024)
	Average elevation	M	https://www.gebco.net (Accessed on 10 September 2024)
	Average slope	°	Calculated using DEM
	Mining area	km^2	Calculated from mine vectors
Economic indicators	Population density	people km^{-2}	http://ghsl.jrc.ec.europa.eu/index.php (Accessed on 10 September 2024)
	Gross domestic product of mining area	billion CNY	Datasets released by Chen and Gao [33]

2.2. Methods

2.2.1. Assessment of the Loss of NEP

In our calculations of the NEP losses in the mining areas, we used the NEP value for 2000 as a reference for each year to calculate the NEP loss per unit area of the mining area. We considered that the change in the NEP of the mining area without mining was similar to the change in the NEP of the area surrounding the mining area, so we took the change in the NEP of the area surrounding the mining area as a reference and characterized the loss of NEP of the mining area as the difference between the change in the reference value and the actual change in the NEP of the mining area. This calculation method can eliminate the influences of the NEP changes caused by environmental factors, and the amount calculated is the NEP loss per unit area, which eliminates the influence of the inequality between the mining area and the surrounding area.

Taking 2001 as an example, the specific calculations are as follows: A and A′ are the NEP values per unit area within the buffer zone of the mining area in 2000 and 2001, respectively, and B and B′ are the NEP values per unit area within the mining area in 2000 and 2001, respectively. A, A′, B, and B′ are used to calculate the value of the change in the NEP per unit area in the mining area and in the buffer zone of the mining area between 2000 and 2001, respectively, after which the difference in the value of the change in the NEP in the buffer zone and the mining area is the loss of NEP in the mining area (Figure 2).

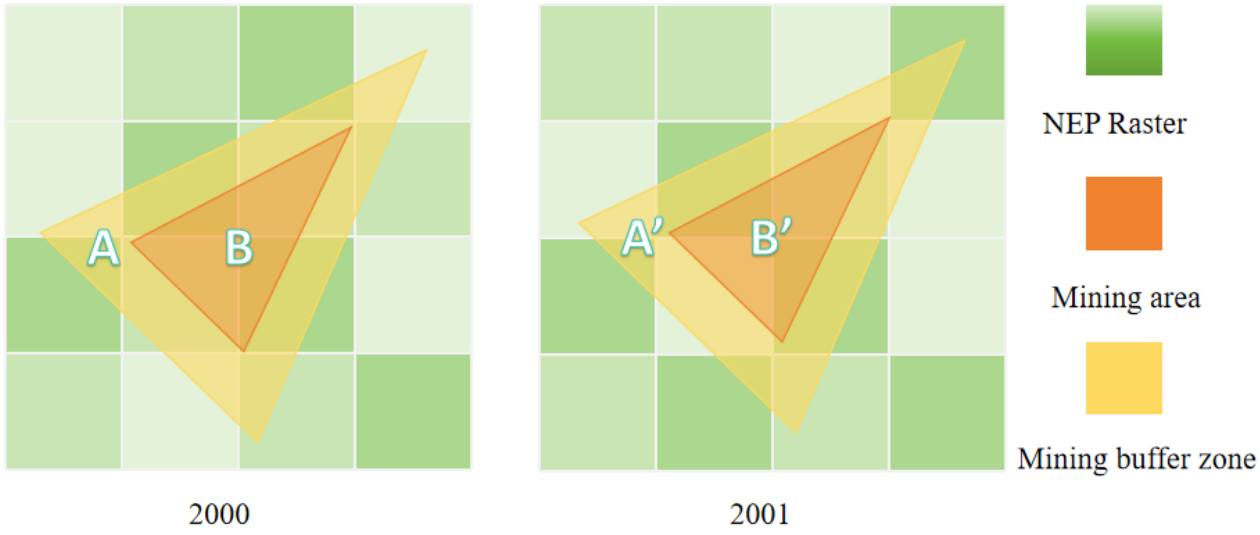


Figure 2. Calculation of the NEP losses per unit area of a mining area.

The formulas used to calculate the NEP losses per unit area for each mining area are as follows:

$$MineChange_t = MineNEP_t - MineNEP_{2000} \quad (1)$$

$$BufferChange_t = BufferNEP_t - BufferNEP_{2000} \quad (2)$$

$$NEPloss_t = BufferChange_t - MineChange_t \quad (3)$$

where t is time, $MineNEP_t$ is the value of the NEP per unit area of the mining area for that year, and $BufferNEP_t$ is the value of the NEP per unit area of the mining area buffer for that year. $MineChange_t$ is the value of the NEP per unit area of the mining area for the change in the NEP from 2000 to t, and $BufferChange_t$ is the amount of NEP per unit area of the mining area buffer for the change in the NEP from 2000 to t. $NEPloss_t$ is the amount of NEP loss per unit area for each mining area from 2000 to t.

The formula used to calculate the total NEP loss of each mining area is as follows:

$$SumLoss_t = NEPloss_t \times AREA \quad (4)$$

where $AREA$ is the area of the mining area, and $SumLoss_t$ is the total NEP loss from 2000 to t for each mining area.

2.2.2. Prediction of the NEP Recovery Potential

NEP recovery potential refers to the amount of NEP could be increased in the mining area. Regarding predicting the recovery potential of the NEP, we vectorized the raster data for the 11 indicators, adding them to a dataset. Because of the poor normality of the data, the data were first transformed into data before sample selection, and we used the Yeo–Johnson data transformation method. The transformation formula is as follows:

$$Y = \begin{cases} log(X+1),\ \lambda = 0, X \geq 0 \\ \frac{(X+1)^{\lambda}-1}{\lambda},\ \lambda \neq 0, X \geq 0 \\ -log(-X+1),\ \lambda = 2, X \leq 0 \\ \frac{-\left[(-X+1)^{(2-\lambda)}-1\right]}{2-\lambda},\ \lambda \neq 2, X \leq 0 \end{cases} \quad (5)$$

where X is the random variable and λ is the transformation coefficient, which can be determined by the great likelihood estimation. Y is the transformed value.

When data processing was complete, we selected 2000 mining areas with NEP increases of greater than 100 g C m^{-2} $year^{-1}$ as a sample set based on the calculation of the NEP losses in the mining areas around the globe. These mining areas represent the highest carbon sequestration that can be achieved by the current practice of environment protection and restoration in mining areas. Then, 85% of the sample set were used as the training set for the model training. During the training, samples from the sample set were selected each time to create the training set. In this manner, multiple tree models were constructed, and the final assessment result was taken as the average of the assessment results of all of the trees, which was used as the NEP recovery potential in the mining area. Moreover, we set parameters such as the number of trees in the forest, the maximum depth of the tree, and the minimum number of samples required to divide the nodes for hyperparameter optimization during the training to obtain the model with the optimal cross-validation (three times) score. Finally, 15% of the samples were used as the validation set for accuracy validation. The root mean square error of the model was calculated. The smaller the root mean square error, the better the prediction performance of the random forest model (Figure 3). In addition, for the 11 driving factors, which had different degrees of importance when assessed using the random forest model, we calculated the importance of each driver by calculating and comparing the conditional replacement importance of all selected predictor variables. The conditional replacement importance was calculated by systematically replacing each predictor variable with a randomized counterpart and measuring the resulting decrease in model accuracy. The higher the value of the conditional replacement importance, the more important is the role of the corresponding predictor variable in predicting NEP. We also used partial dependence plots to visualize the relationship between the target of the variable (i.e., predicted NEP) and each of the important predictor variables [34].

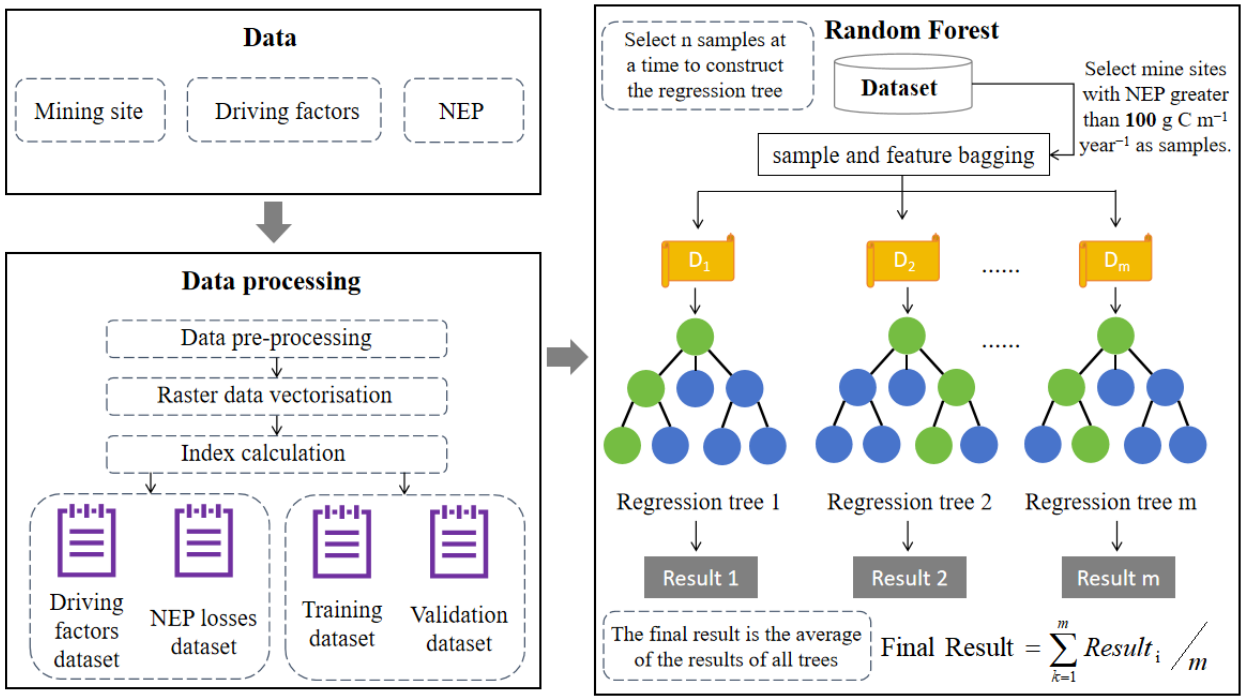


Figure 3. Framework for predicting the NEP recovery potential in the mining areas.

3. Results

3.1. Change in the NEP in the Global Mining Areas During 2000–2020

It was found that from 2000 to 2020, in general, the NEP of the global mining areas exhibited a relatively obvious decreasing trend, with an overall decline of 29.1%, and the highest decline reached 35.7% (Figure 4). In 2001, the NEP of the global mining areas was 2830 Gg, which was the highest value in the 21-year study period, while the lowest value occurred in 2015 when the NEP of the global mining areas was only 1775 Gg. In addition, the change in the NEP in the global mining areas with time was divided into three stages: (1) The period of 2000–2010 was the fluctuation and change stage. During this time period, the linear regression fit R^2 value was 0.16, the global NEP of the mining areas did not exhibit an obvious increasing or decreasing trend, and it always remained above or below 2650 Gg. (2) The period of 2010–2015 was the rapid decline stage. During this time period, the linear regression coefficient reached –0.68, the R^2 value was 0.93, and the NEP of the global mining areas decreased rapidly until it reached the lowest value in 2015. (3) The period of 2015–2020 was the slow recovery stage, during which the NEP of the global mining areas began to recover somewhat, but the amount of recovery was not considerable, and by 2020, it had only recovered to 1955 Gg.

3.2. Loss of NEP in the Global Mining Areas During 2000–2020

Figure 5 shows the NEP losses and gains of the mining areas around the world. The total NEP loss in the global mining areas was 576.9 Gg C year^{-1}. Overall, 52.4% of the mining areas experienced NEP loss, with a total loss of 3555.8 Gg C year^{-1} and an average loss of 144.8 g C m^{-2} year^{-1}. The remaining 47.6% of the mining areas experienced NEP gains of 2978.9 Gg C year^{-1}, with an average gain of 135.6 g C m^{-2} year^{-1}. The histogram in Figure 5 shows that most of the mining areas experienced NEP losses of 200 g C m^{-2} year^{-1}, accounting for 74.0% of the global total, and only a small number of mining areas experienced severe NEP losses or good NEP gains.

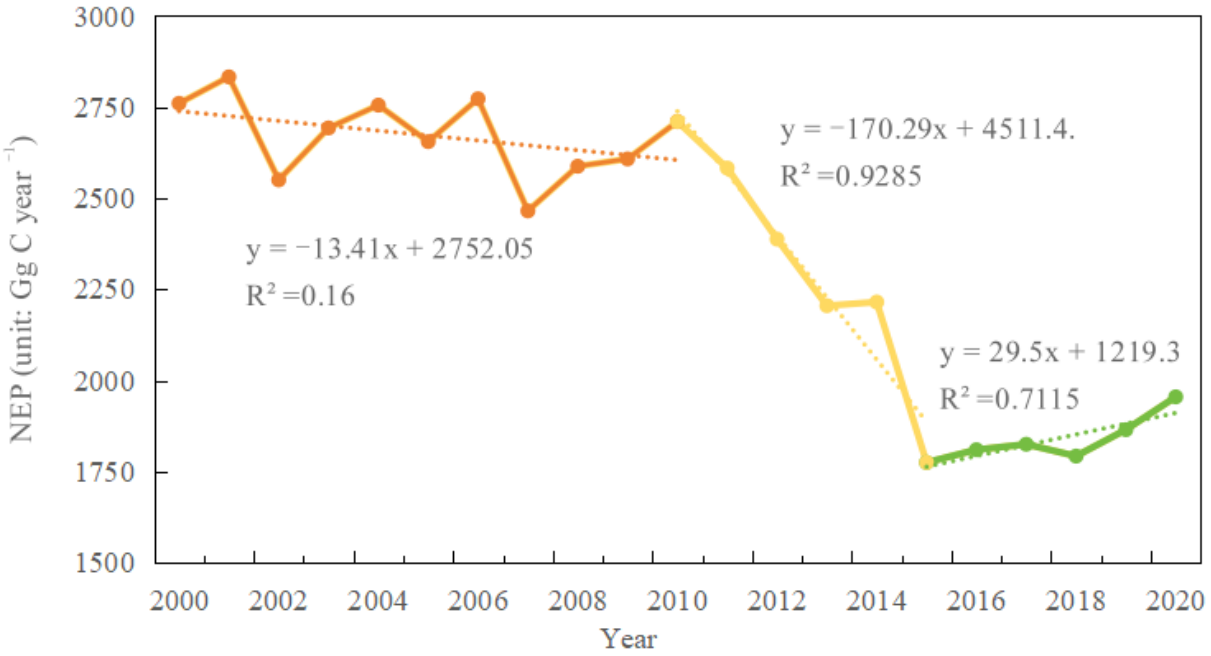


Figure 4. Changes in the NEP in the global mining areas from 2000 to 2020.

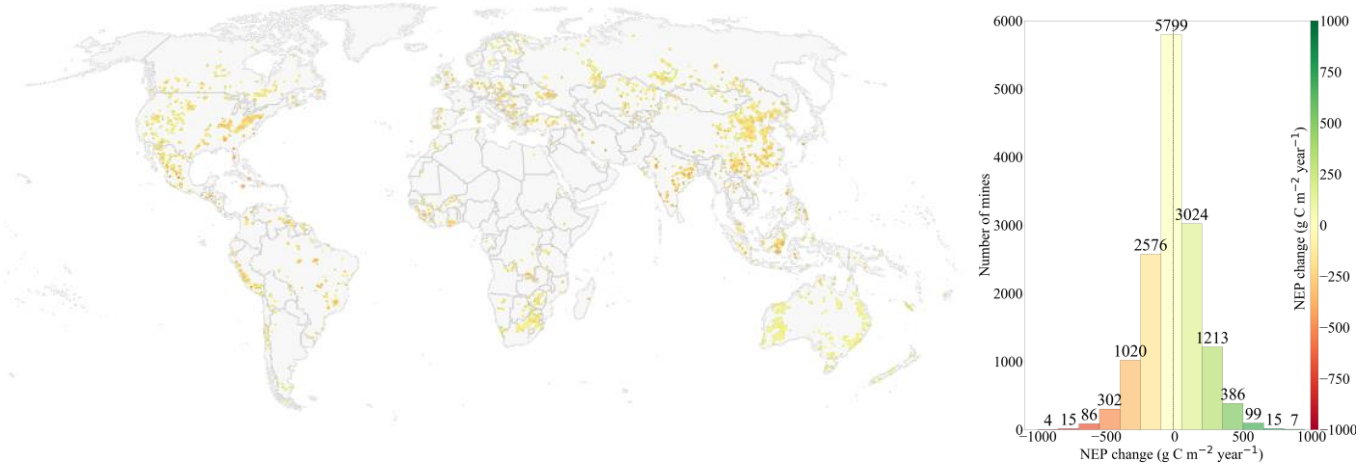


Figure 5. NEP gains and losses of the global mining areas from 2000 to 2020. The negative values denote gains, and the positive values denote losses.

Figure 6 shows the NEP gains and losses of the global mining areas, in which the positive values indicate NEP losses and the negative values indicate NEP gains. It can be seen that from 2001 to 2020, the global mining areas experienced fluctuating gains and losses every year. The maximum value of the loss was 1077.1 g C m^{-2} $year^{-1}$, and the maximum value of the gain was 1060.3 g C m^{-2} $year^{-1}$. Based on the average value of the NEP changes in the global mining areas, their NEP exhibited losses, and the loss value increased, with a loss value of 0.21 g C m^{-2} $year^{-1}$ in 2001. In 2017, it reached the maximum value of 12.4 g C m^{-2} $year^{-1}$, which indicates that the impacts of mining on the NEP of the ecosystems increased from year to year, and from 2017 onward, the loss of the NEP in the mining areas slowed down. By 2020, the average loss of the NEP in the mining areas was 11.9 g C m^{-2} $year^{-1}$.

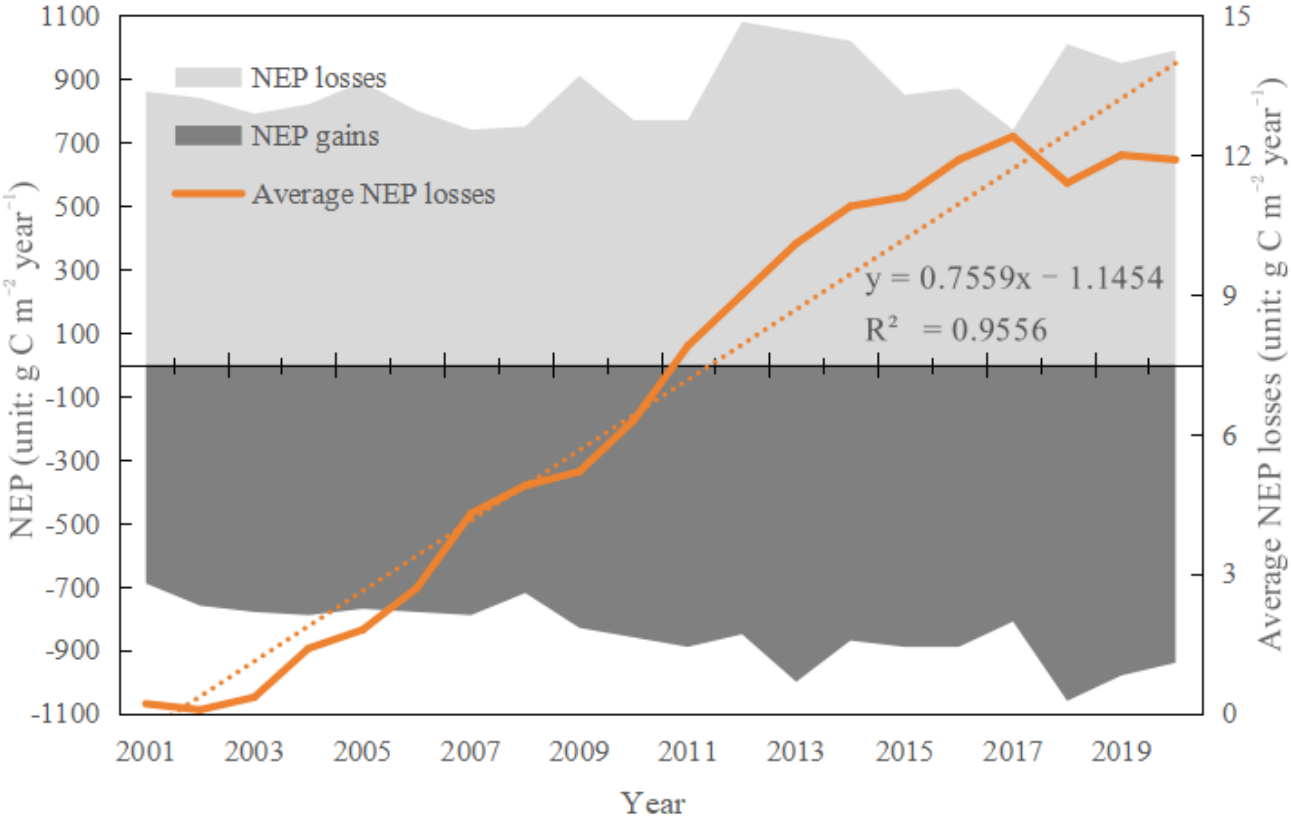


Figure 6. Changes in the average NEP losses in the mining areas from 2000 to 2020 (relative to 2000).

Precipitation is an important factor affecting the vegetation of an area, and areas with good rainfall conditions have higher NEPs. We classified the mining areas with different precipitation conditions into arid mining areas, semi-arid mining areas, semi-humid mining areas, and humid mining areas, analyzed the NEP losses in the different types of mining areas, and calculated their 95% confidence intervals (Figure 7). We analyzed the trends of the average NEP losses in the different types of mining areas. Among the four types of mining areas, the mining areas in the humid zone had the highest NEP losses, which were only lower than those of the other types of mining areas in 2001 and 2015. The increasing trend of the NEP loss was more obvious for the mining areas in the humid zone. The NEP losses in the other three types of mining areas were relatively similar. The changes in the NEP loss in the mining areas in the semi-humid and semi-arid zones were similar, exhibiting small fluctuations, while the mining areas in the arid zone exhibited large fluctuations. In addition, the width of the confidence intervals for the mining areas in the arid zone was significantly larger than those for the mining areas in the other climate zones. This suggests that the NEP losses of the mining areas in the arid zone were more complex and that there was a greater variation in the NEP losses among the mining areas.

Moreover, the NEP losses in these four types of mining areas were relatively similar in 2015, and all of them contained outliers that did not conform to their change trends. The NEP losses in the mining areas in the humid zone decreased significantly, while the NEP losses in the mining areas in the arid zone increased significantly. Except for the outliers in 2015, the NEP losses in the four types of mining areas show that the better the precipitation conditions, the more serious the NEP losses.

However, these anomalies were related to the strong El Niño event in 2015 [35]. This strong El Niño event had a significant impact on the tropical and East Asian subtropical atmospheric circulation, resulting in high precipitation in the equatorial east–central Pacific and central South America and low precipitation in the oceanic continental areas, while many countries in Southeast Asia suffered from severe high temperatures and droughts. This global climate change severely affected the ecosystems and led to large changes in the losses of the NEPs of the mining areas in the climate zones in 2015.

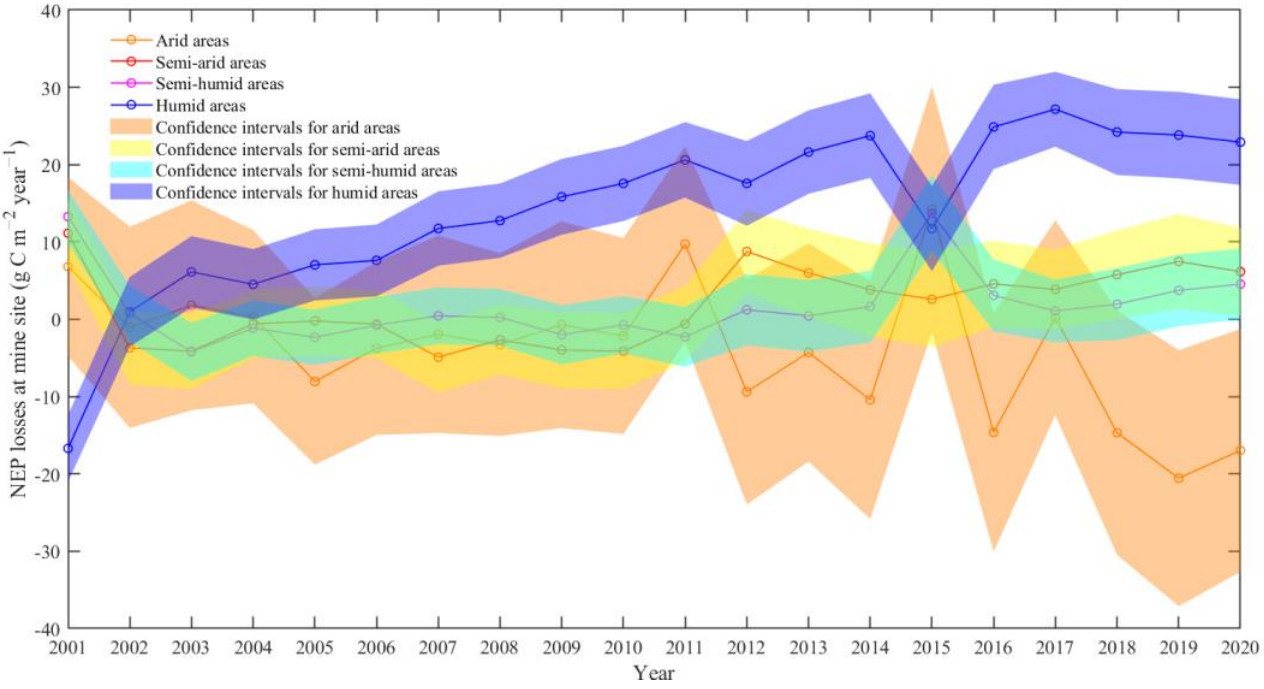


Figure 7. Cumulative NEP losses in mining areas with different rainfall conditions.

3.3. NEP Recovery Potential in Global Mining Areas

The global NEP recovery potential of mines varies greatly (Figure 8), with an average NEP recovery potential of 12.0 g C m^{-2} year^{-1} and a maximum recovery potential of 286.2 g C m^{-2} year^{-1}. Moreover, 40.2% of mines globally have no recovery potential. Table 2 shows the mean value, standard deviation and skewness of the global NEP change and NEP recovery potential for each continent. In Europe, mine site NEP recovery potentials are significantly lower, with most sites having NEP recovery potentials below 10 g C m^{-2} year^{-1}. In contrast, Oceania and South America have significantly higher recovery potentials, with average mine site NEP recovery potentials of 15.9 g C m^{-2} year^{-1} and 16.1 g C m^{-2} year^{-1}, respectively. In Asia, the average mine site recovery potential is 11.4 g C m^{-2} year^{-1}, which is comparable to the global average. However, the recovery potential of the mines in different parts of Asia varies greatly, from a very low average of 5.5 g C m^{-2} year^{-1} in Southeast Asia to 18.6 g C m^{-2} year^{-1} in South Asia, which is a huge difference. In East Asia, which has the densest mining areas in the world, the average recovery potential is 11.1 g C m^{-2} year^{-1}, which is slightly lower than the global average. North America and Africa show the same pattern as Asia, with average recovery potentials of 12.1 g C m^{-2} year^{-1} and 12.3 g C m^{-2} year^{-1}, respectively, but with large spatial variations, with recovery potentials significantly higher in eastern North America than in the west, and significantly higher in southern Africa than in the rest of Africa.

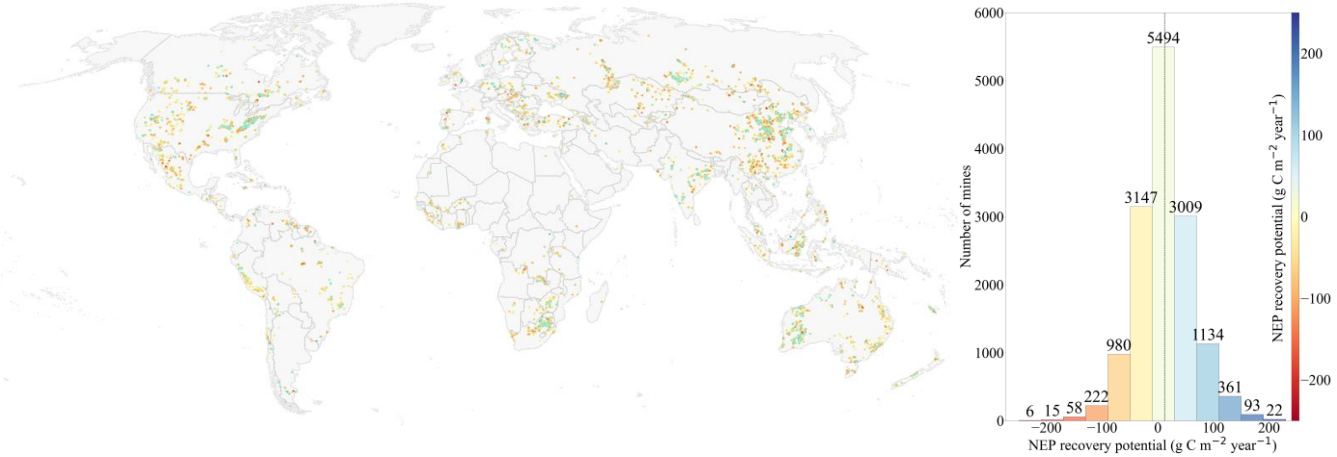


Figure 8. NEP recovery potentials of global mining areas.

Table 2. The mean value, standard deviation and skewness of the global NEP change and NEP recovery potential for each continent.

	Statistics	Asia	Africa	Europe	Oceania	North America	South America
NEP change	Mean value (g C m^{-2} $year^{-1}$)	−14.5	−10.9	5.8	−3.4	−14.4	−28.6
	Standard deviation	203.6	159.5	201.9	52.4	208.6	220.0
	Skewness	0.00	0.23	−0.02	−0.85	−0.06	0.04
NEP recovery potential	Mean value (g C m^{-2} $year^{-1}$)	11.4	12.3	10.6	15.9	12.1	16.1
	Standard deviation	50.2	48.0	48.4	51.8	48.8	50.1
	Skewness	0.08	0.2	0.24	0.38	0.14	0.32

Figure 9 shows the relationship between the predicted values and the true values in the validation set. The random forest model was utilized to predict the NEP recovery potentials of the global mining areas. We evaluated the performance of the random forest model based on the validation set and found that the root mean square error of the evaluation results was 5.59 g C m^{-2} $year^{-1}$ and the R^2 value was 0.8172.

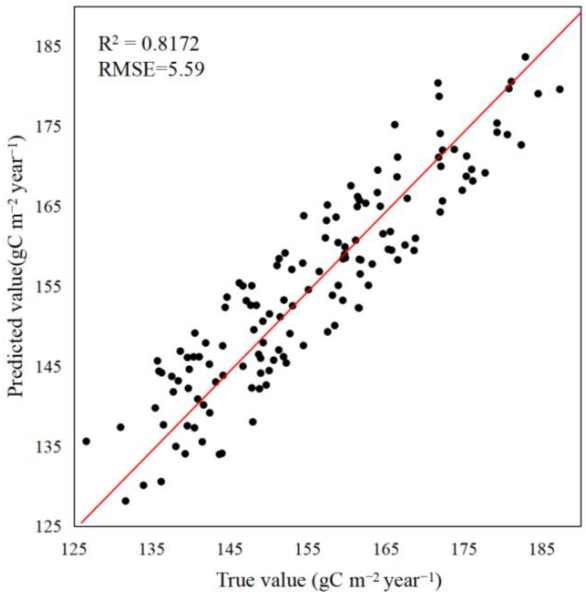


Figure 9. Evaluation of model performance based on the training set and validation set.

3.4. Driving Factors of NEP Recovery in Global Mining Areas

For the 11 driving factors in the random forest model, we calculated the importance of each factor. The results show that (Figure 10) the standardized precipitation evapotranspiration index, population density and the annual precipitation content of the mining area are the main drivers affecting the potential for NEP recovery. The standardized precipitation evapotranspiration index and the annual precipitation represent the water needed for vegetation growth, which is an important indicator of plant growth, and therefore a major driver of NEP restoration in mining areas. Population density, on the other hand, is an important condition for ecological restoration with artificial intervention in mining areas, and also plays an important role in NEP recovery. Meanwhile, gross primary productivity is one of the important indicators of vegetation growth, and thus becomes an important driver of NEP recovery potential in mining areas.

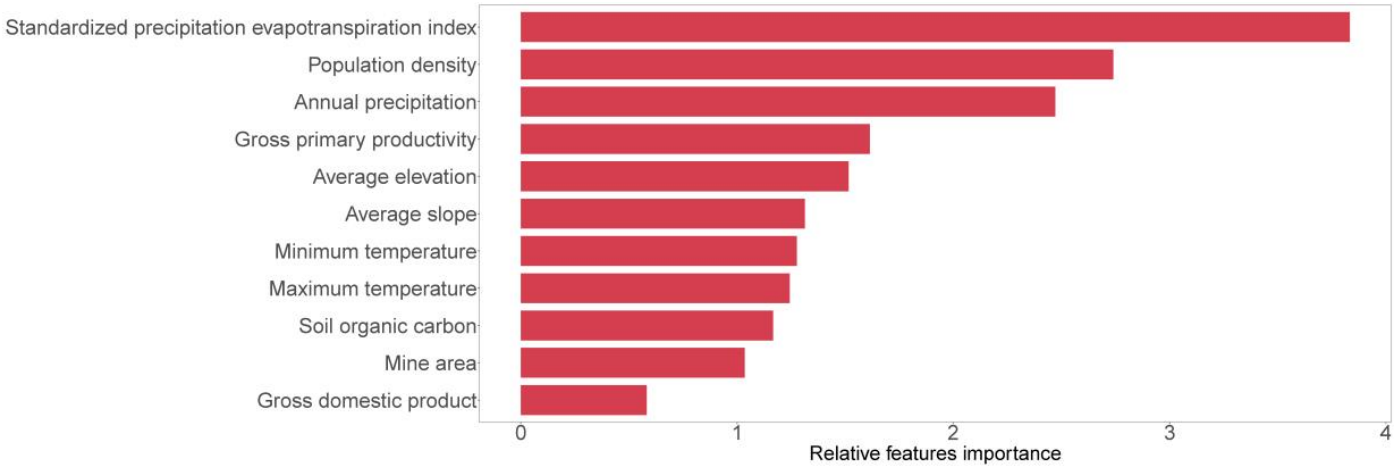


Figure 10. Importance of driving factors.

The partial dependences of the NEP recovery potential of the mining areas on the drivers are shown in Figure 11. Most of the less important drivers did not correlate well with the NEP recovery potential of the mine site. Only standardized precipitation evapotranspiration index, population density, and annual precipitation showed some influential relationship. Among them, the correlation plot of standardized precipitation evapotranspiration index (Figure 11a) shows a "U" shape, indicating that the closer the standardized precipitation evapotranspiration index is to 0, the lower the NEP recovery potential of the mine site is. When the population density is between 0 and 1500 people/km^2, it shows a positive correlation with the recovery potential of the mine site, and the higher the population density, the higher the recovery potential. When the population density reaches 1500/km^2, its contribution to the NEP recovery potential of the mining area reaches saturation (Figure 11b). The correlation of precipitation is similar to that of population density, with an annual precipitation less than 2000 mm showing a positive correlation with the recovery potential of the mine site, reaching saturation at 2000 mm (Figure 11c).

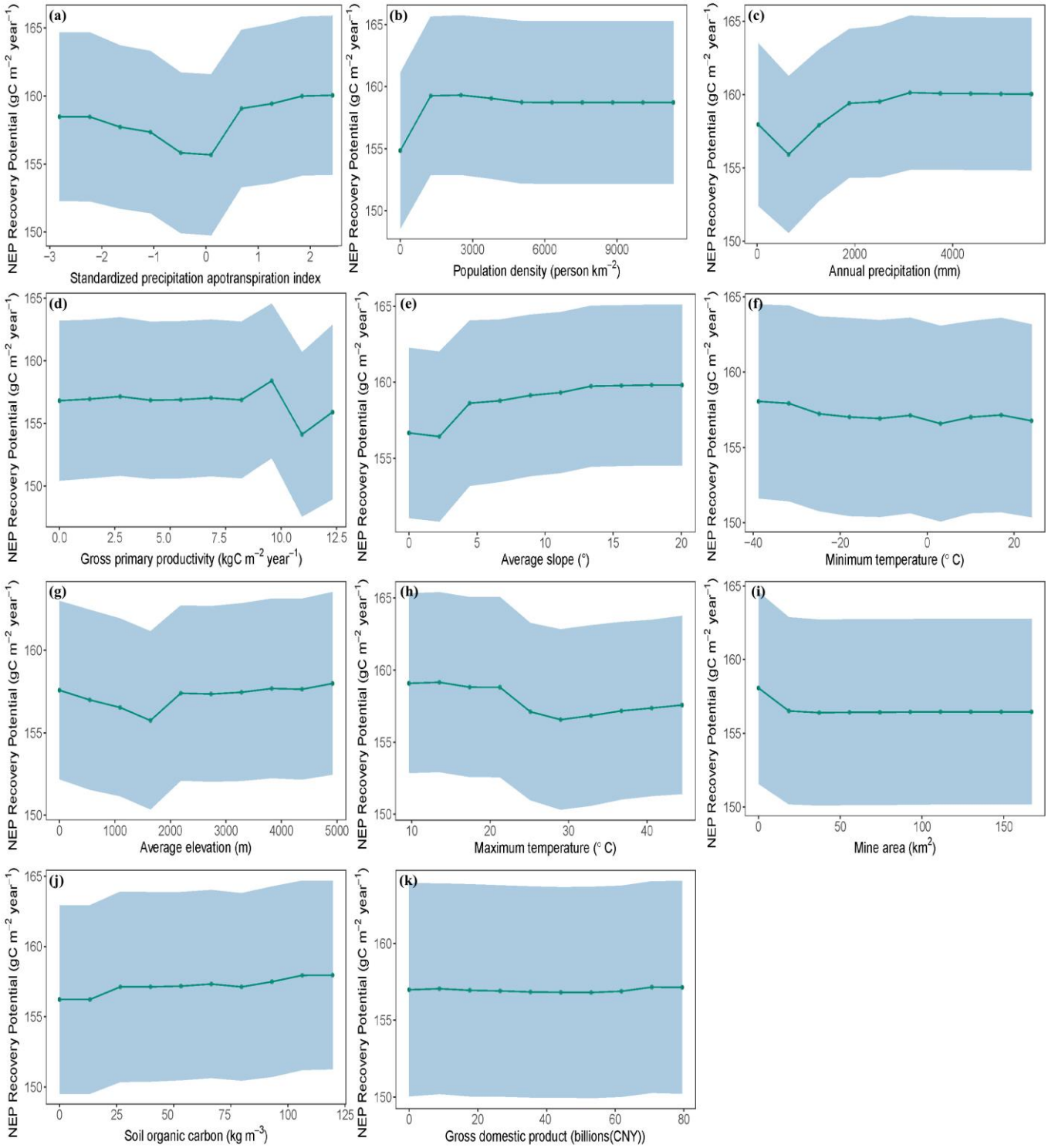


Figure 11. Partial dependency of NEP recovery potential on driving factors: (**a**) Standardized precipitation evapotranspiration index; (**b**) Population density; (**c**) Annual precipitation; (**d**) Average gross primary productivity within the 2 km buffer zone of the mining area; (**e**) Average slope; (**f**) Minimum temperature; (**g**) Average elevation; (**h**) Maximum temperature; (**i**) Area of mining area; (**j**) Soil organic carbon; (**k**) Gross domestic product of mining area.

4. Discussion

4.1. Implications for Mine Ecosystem Management

Mining activities cause extensive damage to global ecosystems not only through physical alterations of the surface but also by leading to NEP significant losses, thereby undermining the carbon sink functions of these areas. Conceptually, ecosystems enhance carbon sequestration by absorbing CO_2 and allocating assimilated carbon to long-lived plant tissues or soil organic matter (SOM) pools where it is protected from microbial decomposition [36]. However, mining activities often result in severe disturbances to terrestrial ecosystems, leading to soil degradation. Enhanced mineralization, as well as increased soil erosion, leaching, mixing, and compaction, diminishes the physical protection against decomposition [37,38], resulting in substantial losses of soil organic carbon. In addition, degraded soils in mining areas tend to be prone to compaction and have low nutrient contents, poor structures, and limited water retention capacities, which restrict soil productivity and thus impede the growth and self-sustainability of vegetation. Moreover, the quantity and quality of the soil organic content, which influences plant productivity, are impacted by vegetation productivity [7,22]. As demonstrated in this study, the rate of NEP loss varied across the different mining areas and primarily depended on the climate conditions and plant species. In the temperate regions, approximately 40% of the carbon accumulated during a 25-year rotation period in plantation forests remained stored in solid wood products. Even young and deteriorating forests can be strong carbon sinks, indicating that temperate forests have a significant potential as atmospheric CO_2 sinks. Based on measurements of the aboveground and belowground biomass in temperate forests, the biomass increase has been estimated to be 4.1 Mg C ha^{-1} $year^{-1}$ [39]. In a reforested area in Canada, in which Jack pine (*Pinus banksiana Lamb*.) plantations were established, historical reclamation practices since the late 1970s have significantly improved the conditions, allowing for the successful establishment of coniferous plantations. The NEPs of revegetated sites are significantly higher than those with the reference conditions, as indicated by the site index, wood volume growth, and ecosystem productivity [40]. A study on an arid region in China revealed that the NEP of a mining area was 781.97 g m^{-2} $year^{-1}$ in 2021, and the forested land served as the primary carbon sink in this mining area [41].

Although mining activities caused extensive damage to ecosystems, we still found that numerous mining regions retained a considerable potential for ecological restoration, particularly in southeastern and southern parts of Asia and parts of East Asia where the NEP restoration potential exceeded the global average. Furthermore, regions with high levels of mining activity, such as the Appalachian Mountains in eastern North America and the Andes in western South America, had considerable restoration potential. However, the variation in NEP recovery potential across different regions may significantly impact the implementation and effectiveness of ecological restoration. Different NEP recovery potentials imply that ecological restoration strategies need to be tailored to local conditions. For instance, in areas with high NEP recovery potential, such as South America and Oceania, restoration strategies can focus more on accelerating natural recovery processes by leveraging the potential carbon sequestration capacities of soil and vegetation to achieve higher rates of carbon fixation [19]. In these areas, significant carbon storage and ecological restoration can be achieved in a short time frame through appropriate plant selection and soil amendment measures. In contrast, in areas with lower NEP recovery potential, such as Europe and Southeast Asia, restoration strategies may need to focus more on improving the physical and chemical properties of the soil to support the re-establishment of vegetation [42]. The soils in mining areas of these regions may be more degraded and recover more slowly, requiring more intensive soil management strategies. For example, it is essential to select plant species tolerant of local soil conditions, apply appropriate fertilization and mulching, and enhance the soil structure to retain moisture and nutrients. Furthermore, as vegetation cover increases, the impact of slope and terrain conditions on vegetation establishment becomes more pronounced. As demonstrated in this study, the successful establishment of vegetation is essential for erosion control, especially on linear

profiles with topsoil cover, where the plant cover is more extensive and uniform. However, in areas with steep slopes, plant establishment is constrained in the upper sections and more favorable in the lower sections. Therefore, in regions with low NEP recovery potential, managing topography (e.g., slope adjustment and optimizing topsoil distribution) should be a key consideration in restoration strategies [43].

These regional differences globally highlight the need for flexibility and specificity in restoration efforts. Areas with high NEP recovery potential may achieve carbon sequestration benefits more quickly, while areas with low NEP recovery potential require more resource inputs and fine-tuned management to overcome limited natural recovery potential. For example, a study in Ohio, USA, demonstrated that systematic reclamation over 25 years allowed pasture soil organic carbon (SOC) stocks to approach the levels found in forest soils and it stabilized earlier than forested lands. This suggests that even in regions with limited NEP recovery potential, SOC levels in reclaimed soils can approach those of natural soils through scientific management [44]. Additionally, research in tropical environments in India showed that CO_2 fluxes in reclaimed mining soils were higher than those in natural woodlands, underscoring the increased soil activity and carbon exchange potential following reclamation [37].The rates of ecosystem carbon sequestration in pine plantations developed on reforested no longer active mining areas in Poland have been reported to range from 1.6 to 5.6 Mg C ha^{-1} $year^{-1}$ [45]. A review of evidence from numerous sites in North America revealed that forest biomass production in reclaimed mineral soils can achieve or even exceed that in natural unmined soils under optimal soil conditions and appropriate management strategies [46,47]. A study conducted in Spain demonstrated that systematic management of the topography and topsoil cover, where the topography influences the pattern of vegetation colonization and the formation of concave slopes, can facilitate successful mine reclamation [48].

In conclusion, the differences in NEP recovery potential across regions indicate that restoration strategies should be adjusted to regional characteristics to effectively promote the recovery of ecological functions in mining areas, maximizing carbon sequestration and ensuring the long-term sustainability of ecosystems. By leveraging identified drivers of NEP recovery potential—soil quality, vegetation type, climate, and topographic conditions—restoration strategies can be optimized to enhance recovery outcomes and establish resilient ecosystems that support long-term carbon sequestration and biodiversity conservation. This approach aligns closely with Sustainable Development Goals (SDGs), particularly SDG 13 (Climate Action) and SDG 15 (Life on Land), as it emphasizes ecosystem restoration and carbon sequestration in degraded mining areas to mitigate climate change impacts. Additionally, incorporating these strategies into mining management policies can support SDG 12 (Responsible Consumption and Production) by promoting sustainable practices within the mining sector. Our findings provide a scientific basis for policies that prioritize ecosystem resilience and carbon balance in post-mining landscapes, helping policymakers develop regionally tailored restoration standards that enhance biodiversity and ecosystem functionality. By advancing these strategies, the mining sector can better contribute to global sustainability goals and more effectively manage the environmental impacts associated with resource extraction.

4.2. Limitations and Future Work

In this study, we focused on the loss and recovery potential of NEP in global mining areas. The dataset used was generated by visually interpreting Sentinel-2 images acquired in 2019 [27]. This effort resulted in a comprehensive global dataset. Although significantly expanded, the dataset still does not encompass all existing mines globally as we only considered areas within a 10 km buffer around the coordinates provided by the SNL Metals and Mining dataset (https://www.marketplace.spglobal.com/) (Accessed on 10 September 2024). This dataset does not include data on how long the mines have been in operation, and the relevant environmental regulations followed in their operation varied from one period to the next. Furthermore, the mine closure time was not emphasized in

most early mining planning. However, studies have shown that considering the mine closure time in mine planning can minimize additional environmental damage [49]. Thus, the time of operation of a mine is also a major factor affecting its recovery potential. Moreover, the underlying data introduce some uncertainty. The NEP data have a limited temporal coverage, which is crucial for assessing NEP losses. In addition, the limited spatial resolution of the data used to assess the recovery potential and the small sizes of most of the mines impacted the accuracy of the calculations of the drivers within the mining areas. The absence of ground validation data on the actual recovery potential also contributed to the uncertainty. Another limitation of this study is the lack of a direct comparison between NEP changes in mining areas and natural ecosystem variability or non-mining regions. In non-mining ecosystems, NEP variations are primarily influenced by natural factors such as climate fluctuations, vegetation succession, and soil dynamics, whereas in mining areas, the substantial disturbances caused by extraction activities lead to abrupt NEP declines and altered recovery trajectories. Additionally, confounding factors such as climate change and surrounding land-use changes could indirectly affect NEP trends in mining areas by influencing local climate, soil, and vegetation conditions. Future studies could further clarify these dynamics by integrating broader environmental data to mining's impacts on NEP.

Future work should focus on improving the data sources and strengthening long-term monitoring to broaden the time series data used in analyses, which can encompass the entire period of operation of a mine if accurate NEP losses from mineral extraction are to be obtained. The NEP loss can be more accurately calculated by integrating the duration of the mine operation into the assessment. In addition, in the future, high-resolution remote sensing data will be employed to improve the precision of our findings. The type of mine is another important influencing factor that needs to be considered. Furthermore, the currently available global mining data only categorizes mines as coal and metal, and we lack data on specific metal types (such as rare metals and precious metals). As a result, we were unable to conduct a comparison for different types of mines. Therefore, we believe that future research should focus on developing more detailed datasets to enable a thorough classification and evaluation of the ecological impacts associated with various types of mines. Moreover, future studies could enhance understanding of these dynamics by integrating broader environmental data, such as climate and land-use variables, to better identify the specific impacts of mining on NEP and to compare them with natural ecosystem trends. This approach would provide a more comprehensive view of the unique challenges in restoring NEP in mining areas and support targeted restoration strategies.

5. Conclusions

In this study, we analyzed global terrestrial mining areas and their NEP changes, calculated the NEP losses in these areas, and utilized a random forest model to assess the NEP recovery potential and its drivers. Our results provide a scientific basis for the ecological restoration and sustainable development of global mining areas. The conclusions of this study are summarized below.

Between 2000 and 2020, the NEP in global mining areas exhibited a relatively obvious decreasing trend, with a decline of 29.1% and a maximum decline of 35.7%. NEP loss occurred in 52.4% of the global mining areas, and the amount of NEP loss exhibited a clearly increasing trend. By 2020, the NEP loss in the mining areas was 11.9 g C m^{-2} $year^{-1}$, and the total loss reached 576.9 Gg C $year^{-1}$. The NEP loss exhibited different trends in areas with different precipitation conditions, and mining areas with more precipitation experienced more serious NEP loss.

It was found that the global mining areas had remarkable NEP recovery potentials, and the average NEP recovery potential of the global mining areas was 12.0 g C m^{-2} $year^{-1}$. The standardized precipitation evapotranspiration index, population density, and the annual precipitation were the most important drivers.

The ecological restoration of mines is of great importance for the recovery of NEP and thus the enhancement of ecosystem carbon pools. The results of this study demonstrate that on the global scale, mines have a significant carbon sequestration potential. However, the factors that influence the potential of carbon sinks in reclaimed mining areas require further investigation. Furthermore, the long-term impacts of ecological restoration on the NEP remain unclear, and the long-term NEP of reclaimed mining areas needs to be studied to identify sustainable management options.

Author Contributions: Conceptualization, experiment design, investigation, and writing, Y.Y., Q.W. and R.G.; methodology, validation, formal analysis, and software, Y.Y., R.G. and F.C.; funding acquisition and resources, Y.Y. and S.L.; supervision and project administration, F.C. All authors have read and agreed to the published version of the manuscript.

Funding: This work was supported by the National Key Research and Development Program of China (2023YFF1306005), the National Natural Science Foundation of China (52474197), and the Jiangsu Province Natural Resources Science and Technology Innovation Project (2023034).

Data Availability Statement: The raw data supporting the conclusions of this article will be made available by the authors on request.

Conflicts of Interest: The authors declare no conflicts of interest.

References

1. Buotte, P.C.; Law, B.E.; Ripple, W.J.; Berner, L.T. Carbon sequestration and biodiversity co-benefits of preserving forests in the western United States. *Ecol. Appl.* **2020**, *30*, e02039. [CrossRef] [PubMed]
2. Calvin, K.; Dasgupta, D.; Krinner, G.; Mukherji, A.; Thorne, P.W.; Trisos, C.; Romero, J.; Aldunce, P.; Barrett, K.; Blanco, G.; et al. *2023: Climate Change 2023: Synthesis Report. Contribution of Working Groups I, II and III to the Sixth Assessment Report of the Intergovernmental Panel on Climate Change*; Core Writing Team, Lee, H., Romero, J., Eds.; Intergovernmental Panel on Climate Change (IPCC): Geneva, Switzerland, 2023.
3. de Chazournes, L.B. *Kyoto Protocol to the United Nations Framework Convention on Climate Change*; Kyoto Protocol: Kyoto, Japan, 1997.
4. Lyu, J.; Fu, X.; Lu, C.; Zhang, Y.; Luo, P.; Guo, P.; Huo, A.; Zhou, M. Quantitative assessment of spatiotemporal dynamics in vegetation NPP, NEP and carbon sink capacity in the Weihe River Basin from 2001 to 2020. *J. Clean. Prod.* **2023**, *428*, 139384. [CrossRef]
5. Mohamed, M.A.A.; Babiker, I.S.; Chen, Z.M.; Ikeda, K.; Ohta, K.; Kato, K. The role of climate variability in the inter-annual variation of terrestrial net primary production (NPP). *Sci. Total Environ.* **2004**, *332*, 123–137. [CrossRef] [PubMed]
6. Locatelli, F.; Fishbane, S.; Block, G.A.; Macdougall, I.C. Targeting Hypoxia-Inducible Factors for the Treatment of Anemia in Chronic Kidney Disease Patients. *Am. J. Nephrol.* **2017**, *45*, 187–199. [CrossRef]
7. Zhao, J.; Ma, J.; Zhu, Y. Evaluating impacts of climate change on net ecosystem productivity (NEP) of global different forest types based on an individual tree-based model FORCCHN and remote sensing. *Glob. Planet. Chang.* **2019**, *182*, 103010. [CrossRef]
8. Zhang, C.; Bai, Q.; Han, P. A review of water rock interaction in underground coal mining: Problems and analysis. *Bull. Eng. Geol. Environ.* **2023**, *82*, 157. [CrossRef]
9. Xu, D.; Zhao, Y.; Jiang, Y.; Zhang, C.; Sun, B.; He, X. Using improved edge detection method to detect mining-induced ground fissures identified by unmanned aerial vehicle remote sensing. *Remote Sens.* **2021**, *13*, 3652. [CrossRef]
10. Krzyszowska, W.A. Sustainable reclamation practices for a large surface coal mine in shortgrass prairie, semiarid environment (Wyoming, USA): Case study. *Int. J. Coal Sci. Technol.* **2022**, *9*, 32. [CrossRef]
11. Townsend, P.A.; Helmers, D.P.; Kingdon, C.C.; McNeil, B.E.; de Beurs, K.M.; Eshleman, K.N. Changes in the extent of surface mining and reclamation in the Central Appalachians detected using a 1976–2006 Landsat time series. *Remote Sens. Environ.* **2009**, *113*, 62–72. [CrossRef]
12. Butt, N.; Beyer, H.L.; Bennett, J.R.; Biggs, D.; Maggini, R.; Mills, M.; Renwick, A.R.; Seabrook, L.M.; Possingham, H.P. Biodiversity Risks from Fossil Fuel Extraction. *Science* **2013**, *342*, 425–426. [CrossRef]
13. Harfoot, M.B.J.; Tittensor, D.P.; Knight, S.; Arnell, A.P.; Blyth, S.; Brooks, S.; Butchart, S.H.M.; Hutton, J.; Jones, M.I.; Kapos, V.; et al. Present and future biodiversity risks from fossil fuel exploitation. *Conserv. Lett.* **2018**, *11*, e12448. [CrossRef]
14. Owen, J.R.; Kemp, D. Mining-induced displacement and resettlement: A critical appraisal. *J. Clean. Prod.* **2015**, *87*, 478–488. [CrossRef]
15. Yang, Y.; Dong, J.; Tang, J.; Zhao, J.; Lei, S.; Zhang, S.; Chen, F. Mapping Foliar C, N, and P Concentrations in An Ecological Restoration Area with Mixed Plant Communities Based on LiDAR and Hyperspectral Data. *Remote Sens.* **2024**, *16*, 1624. [CrossRef]
16. Latifovic, R.; Fytas, K.; Chen, J.; Paraszczak, J. Assessing land cover change resulting from large surface mining development. *Int. J. Appl. Earth Obs. Geoinf.* **2005**, *7*, 29–48. [CrossRef]

17. Waring, R.H.; Coops, N.C.; Running, S.W. Predicting satellite-derived patterns of large-scale disturbances in forests of the Pacific Northwest Region in response to recent climatic variation. *Remote Sens. Environ.* **2011**, *115*, 3554–3566. [CrossRef]
18. Ma, Q.; He, C.; Fang, X. A rapid method for quantifying landscape-scale vegetation disturbances by surface coal mining in arid and semiarid regions. *Landsc. Ecol.* **2018**, *33*, 2061–2070. [CrossRef]
19. Qiu, S.; Yu, Q.; Niu, T.; Fang, M.; Guo, H.; Liu, H.; Li, S.; Zhang, J. Restoration and renewal of ecological spatial network in mining cities for the purpose of enhancing carbon Sinks: The case of Xuzhou, China. *Ecol. Indic.* **2022**, *143*, 109313. [CrossRef]
20. Xu, Z.; Hou, H.; Zhang, S.; Ding, Z.; Ma, C.; Gong, Y.; Liu, Y. Effects of mining activity and climatic change on ecological losses in coal mining areas. *Trans. Chin. Soc. Agric. Eng.* **2012**, *28*, 232–240.
21. Hou, H.; Zhang, S.; Ding, Z.; Gong, Y.; Ma, C. Study on the measurement of ecological loss based on the net primary productivity in coal mines. *J. China Coal Soc.* **2012**, *37*, 445–451.
22. Sonter, L.J.; Dade, M.C.; Watson, J.E.M.; Valenta, R.K. Renewable energy production will exacerbate mining threats to biodiversity. *Nat. Commun.* **2020**, *11*, 4174. [CrossRef]
23. Akala, V.A.; Lal, R. Potential of Mine Land Reclamation for Soil Organic Carbon Sequestration in Ohio. *Land Degrad. Dev.* **2000**, *11*, 289–297. [CrossRef]
24. Chen, F.; Zhu, Y.; Bi, Y.; Yang, Y.; Ma, J.; Peng, S. High-priority actions to improve carbon sequestration potential for mining ecological restoration in China. *Engineering*. 2024, *in press*. [CrossRef]
25. Werner, T.T.; Mudd, G.M.; Schipper, A.M.; Huijbregts, M.A.J.; Taneja, L.; Northey, S.A. Global-scale remote sensing of mine areas and analysis of factors explaining their extent. *Glob. Environ. Chang.* **2020**, *60*, 102007. [CrossRef]
26. Maus, V.; Giljum, S.; Gutschlhofer, J.; da Silva, D.M.; Probst, M.; Gass, S.L.B.; Luckeneder, S.; Lieber, M.; McCallum, I. A global-scale data set of mining areas. *Sci. Data* **2020**, *7*, 289. [CrossRef]
27. Maus, V.; Giljum, S.; da Silva, D.M.; Gutschlhofer, J.; da Rosa, R.P.; Luckeneder, S.; Gass, S.L.B.; Lieber, M.; McCallum, I. An update on global mining land use. *Sci. Data* **2022**, *9*, 433. [CrossRef]
28. Huang, N.; Wang, L.; Zhang, Y.L.; Gao, S.; Niu, Z. Estimating the net ecosystem exchange at global FLUXNET sites using a random forest model. *J. Sel. Top. Appl. Earth Obs. Remote Sens.* **2021**, *14*, 9826–9836. [CrossRef]
29. Beguería, S.; Vicente Serrano, S.M.; Reig-Gracia, F.; Latorre Garcés, B. *SPEIbase*, Version 2.8; DIGITAL.CSIC.; Spanish National Research Council: Madrid, Spain, 2023.
30. Wild, B.; Teubner, I.; Mösinger, L.; Zotta, R.-M.; Forkel, M.; van der Schalie, R.; Sitch, S.; Dorigo, W.A. VODCA2GPP—A new, global, long-term (1988–2020) gross primary production dataset from microwave remote sensing. *Earth Syst. Sci. Data* **2021**, *14*, 1063–1085. [CrossRef]
31. Teubner, I.E.; Forkel, M.; Camps-Valls, G.; Jung, M.; Miralles, D.G.; Tramontana, G.; van der Schalie, R.; Vreugdenhil, M.; Mösinger, L.; Dorigo, W.A. A carbon sink-driven approach to estimate gross primary production from microwave satellite observations. *Remote Sens. Environ.* **2019**, *229*, 100–113. [CrossRef]
32. Teubner, I.E.; Forkel, M.; Wild, B.; Mösinger, L.; Dorigo, W. Impact of temperature and water availability on microwave-derived gross primary production. *Biogeosci. Discuss.* **2020**, *18*, 3285–3308. [CrossRef]
33. Chen, J.; Gao, M.; Cheng, S.; Hou, W.; Song, M.; Liu, X.; Liu, Y. Global 1 km × 1 km gridded revised real gross domestic product and electricity consumption during 1992–2019 based on calibrated nighttime light data. *Sci. Data* **2022**, *9*, 202. [CrossRef]
34. Le, T.D.H.; Kattwinkel, M.; Schützenmeister, K.; Olson, J.R.; Hawkins, C.P.; Schäfer, R.B. Predicting current and future background ion concentrations in German surface water under climate change. *Philos. Trans. R. Soc. B Biol. Sci.* **2018**, *374*, 20180004. [CrossRef] [PubMed]
35. Zhai, P.; Yu, R.; Guo, Y.; Li, Q.; Ren, X.; Wang, Y.; Xu, W.; Liu, Y.; Ding, Y. The strong El Niño of 2015/16 and its dominant impacts on global and China's climate. *J. Meteorol. Res.* **2016**, *30*, 283–297. [CrossRef]
36. Wei, X.; Yang, J.; Luo, P.; Lin, L.; Lin, K.; Guan, J. Assessment of the variation and influencing factors of vegetation NPP and carbon sink capacity under different natural conditions. *Ecol. Indic.* **2022**, *138*, 108834. [CrossRef]
37. Ahirwal, J.; Maiti, S.K.; Singh, A.K. Changes in ecosystem carbon pool and soil CO_2 flux following post-mine reclamation in dry tropical environment, India. *Sci. Total Environ.* **2017**, *583*, 153–162. [CrossRef] [PubMed]
38. Chen, F.; Zhu, Y.; Ma, J.; Dong, W.; You, Y.; Yang, Y. Mechanism, potential and regulation of carbon sequestration and sink enhancement in ecological restoration of mining areas in the Loess Plateau. *Coal Sci. Technol.* **2023**, *51*, 502–513.
39. Winjum, J.K.; Schroeder, P.E. Forest plantations of the world: Their extent, ecological attributes, and carbon storage. *Agric. For. Meteorol.* **1997**, *84*, 153–167. [CrossRef]
40. Metsaranta, J.M.; Beauchemin, S.; Langley, S.; Tisch, B.; Dale, P. Assessing the long-term ecosystem productivity benefits and potential impacts of forests re-established on a mine tailings site. *Forests* **2018**, *9*, 707. [CrossRef]
41. Chen, F.; Liu, Y.; Guo, J.; Bai, H.; Wu, Z.; Liu, Y.; Li, R. Assessing Carbon Sink Capacity in Coal Mining Areas: A Case Study from Taiyuan City. *China Atmos.* **2024**, *15*, 765. [CrossRef]
42. Adeli, A.; Brooks, J.P.; Read, J.J.; McGrew, R.; Jenkins, J.N. Post-reclamation Age Effects on Soil Physical Properties and Microbial Activity Under Forest and Pasture Ecosystems. Commun. *Soil Sci. Plant Anal.* **2019**, *50*, 20–34. [CrossRef]
43. Duque, J.F.M.; Pedraza, J.; Díez, A.; Sanz, M.A.; Carrasco, R.M. A geomorphological design for the rehabilitation of an abandoned sand quarry in central Spain. *Landsc. Urban Plan.* **1998**, *42*, 1–14. [CrossRef]
44. Ussiri, D.A.N.; Lal, R. Carbon Sequestration in Reclaimed Minesoils. *Crit. Rev. Plant Sci.* **2005**, *24*, 151–165. [CrossRef]

45. Pietrzykowski, M.; Daniels, W.L. Estimation of carbon sequestration by pine (*Pinus sylvestris* L.) ecosystems developed on reforested post-mining sites in Poland on differing mine soil substrates. *Ecol. Eng.* **2014**, *73*, 209–218. [CrossRef]
46. Ussiri, D.A.N.; Guzman, J.G.; Lal, R.; Somireddy, U. Bioenergy crop production on reclaimed mine land in the North Appalachian region, USA. *Biomass Bioenergy* **2019**, *125*, 188–195. [CrossRef]
47. Zipper, C.E.; Burger, J.A.; Barton, C.D.; Skousen, J.G. Rebuilding Soils on Mined Land for Native Forests in Appalachia. *Soil Sci. Soc. Am. J.* **2013**, *77*, 337–349. [CrossRef]
48. Martín-Moreno, C.; Martín Duque, J.F.; Nicolau Ibarra, J.M.; Hernando Rodríguez, N.; Sanz Santos, M.Á.; Sánchez Castillo, L. Effects of Topography and Surface Soil Cover on Erosion for Mining Reclamation: The Experimental Spoil Heap at El Machorro Mine (Central Spain). *Land Degrad. Dev.* **2016**, *27*, 145–159. [CrossRef]
49. Nehring, M.; Cheng, X. An investigation into the impact of mine closure and its associated cost on life of mine planning and resource recovery. *J. Clean. Prod.* **2016**, *127*, 228–239. [CrossRef]

Disclaimer/Publisher's Note: The statements, opinions and data contained in all publications are solely those of the individual author(s) and contributor(s) and not of MDPI and/or the editor(s). MDPI and/or the editor(s) disclaim responsibility for any injury to people or property resulting from any ideas, methods, instructions or products referred to in the content.